ChemComm

COMMUNICATION

View Article Online
View Journal | View Issue

Open Access Article. Published on 27 May 2014. Downloaded on 7/24/2025 2:59:40 AM.
This article is licensed under a Creative Commons Attribution 3.0 Unported Licence.

Cite this: *Chem. Commun.*, 2014, 50, 8484

Received 2nd April 2014,
Accepted 23rd May 2014

DOI: 10.1039/c4cc02442g

www.rsc.org/chemcomm

Synergistic acceleration in the osteogenesis of human mesenchymal stem cells by graphene oxide–calcium phosphate nanocomposites†

Rameshwar Tatavarty,[a] Hao Ding,[a] Guijin Lu,[a] Robert J. Taylor[b] and Xiaohong Bi*[a]

Nanocomposites consisting of oblong ultrathin plate shaped calcium phosphate nanoparticles and graphene oxide microflakes were synthesized and have demonstrated markedly synergistic effect in accelerating stem cell differentiation to osteoblasts.

Stem cells (SCs) including mesenchymal, embryonic and induced pluripotent SCs possess the potential to differentiate toward multiple lineages such as bone, fat, and muscle, and therefore offer promising opportunities for developing SCs-based regenerative therapy and tissue engineering. However, to fully exploit the application of SCs in tissue regeneration, it is critical to develop biochemical, chemical, or physical factors that can control the self-renewal and differentiation of SCs toward the desired lineage. Recently, graphene family nanomaterials such as graphene (G) and graphene oxide (GO) attracted substantial interest as new platforms for SCs-based biomedical applications, because of their physicochemical properties, distinctive nanostructure, and outstanding mechanical properties. Both materials, especially GO with more hydrophilic surface, promote cell adhesion, proliferation, and differentiation.[1] Substrates coated with G or GO demonstrated the capability of facilitating SCs differentiation toward multiple specific lineages.[2] Enhanced osteogenesis, adipogenesis, and epithelial genesis in various SCs have been reported on GO coated surface,[3] suggesting G and GO as promising base materials for building scaffolds and composites for SCs-based tissue engineering.

Here we hypothesized that incorporating GO with an osteoinductive material could synergistically direct the differentiation of human mesenchymal stem cells (hMSCs) toward osteogenic lineage. Calcium phosphates (CaP) such as hydroxyapatite (HAp) are biomimetic biomaterials that are well-recognized for their osteoconductivity (facilitating bone formation) and osteoinductivity (facilitating the osteogenic differentiation of hMSCs).[4] To validate the above hypothesis, we synthesized a novel biocompatible GO–CaP nanocomposite and evaluated its capability of inducing the osteogenic differentiation in hMSCs. The GO–CaP nanocomposite was fabricated using GO microflakes, uniquely structured highly osteoinductive CaP nanoparticles, and Pluronic® polymeric coating. The osteoinductive properties of GO microflakes, CaP, and GO–CaP on hMSCs were evaluated by quantitative measurements on bone nodule formation and the immunofluorescence imaging of osteoblast biomarkers. GO–CaP exhibited osteogenic capability that was superior to individual or combined effects of GO and CaP.

The fabrication process of GO–CaP nanocomposite is illustrated in Fig. 1. Pluronic® F127 coated GO–CaP and CaP (referred as GO–CaP and CaP in the following texts) were synthesized *via* a double-reverse microemulsion method modified from previous report.[5] Detailed procedures are described in ESI.† Once fabricated,

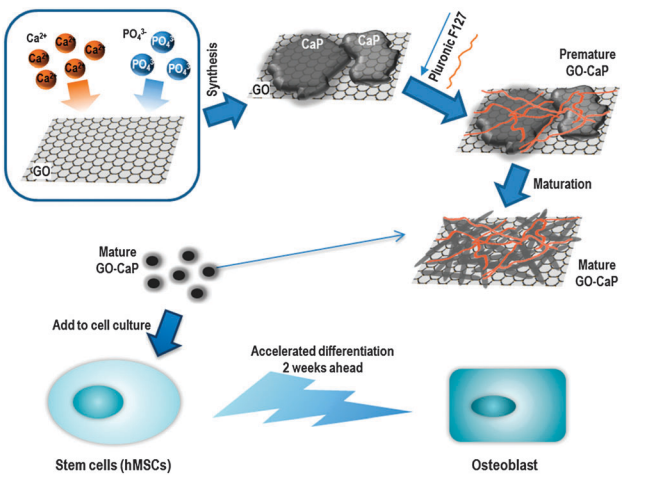

Fig. 1 Schematic illustration of fabrication procedure for GO–CaP nanocomposites, and subsequent synergistic acceleration of osteogenesis in hMSCs by GO–CaP.

[a] *Department of Nanomedicine and Biomedical Engineering, the University of Texas Health Science Center at Houston, 1881 East Road, Houston, TX 77054, USA. E-mail: Xiaohong.bi@uth.tmc.edu*

[b] *Department of Veterinary Integrative Biosciences, Texas A&M University, College Station, TX 77843-4458, USA*

† Electronic supplementary information (ESI) available: Experimental details and supplementary figures. See DOI: 10.1039/c4cc02442g

This journal is © The Royal Society of Chemistry 2014

Open Access Article. Published on 27 May 2014. Downloaded on 7/24/2025 2:59:40 AM.
This article is licensed under a Creative Commons Attribution 3.0 Unported Licence.

the particles were stored in deionized water for 2 to 3 weeks to allow for crystal maturation. The maturation process is an essential procedure to obtain the highly osteoinductive nanoparticles in this study.

The relative weight percentage of GO flakes and CaP nanoparticles in the recipe of the nanocomposites was determined by analysing the cytotoxicity of each individual component. The cytotoxicity of GO and CaP was evaluated by measuring the cell viability of hMSCs after 3 days of incubation with different particle dosages using the colorimetric MTT assay (Fig. S1 in ESI†). With neutralized GO, the cell viability of hMSCs remained above 60% when the final concentration of GO in the culture medium was ≤ 1 μg ml^{-1}, and fell sharply to $<20\%$ at concentrations above 10 μg ml^{-1} (Fig. S1A, ESI†). CaP nanoparticles demonstrated remarkable biocompatibility with $>75\%$ viability when final concentration is ≤ 50 μg ml^{-1} (Fig. S1B, ESI†). Based on these outcomes, the optimal recipe for GO–CaP nanocomposite was determined to be 0.5 μg ml^{-1} GO and 10 μg ml^{-1} calcium phosphate, or a weight ratio of 1 : 20. Cell viability with GO–CaP treatment was above 80% with 10.5 μg ml^{-1} GO–CaP particles (Fig. S1C, ESI†). To achieve the highest osteogenesis while maintaining the most cell viability, 10.5 μg ml^{-1} GO–CaP was determined for the differentiation of hMSCs in the present study. For valid comparison, we used GO and CaP at the same concentration as their presence in GO–CaP, *i.e.* 0.5 μg ml^{-1} GO and 10 μg ml^{-1} CaP for all the following tests.

The structural morphology of GO, CaP and GO–CaP was investigated using transmission electron microscopy (TEM). The GO microflakes were commercially purchased (Nanocs Inc, New York, NY) with a size of 0.5–5 microns. Over 80% of the flakes consist of a single atomic layer. CaP nanoparticles exhibited an irregular plate shape when freshly made (Fig. S2A-I, ESI†), gradually separated and elongated to rod-shaped platelets in a week (Fig. S2A-II, ESI†), and stabilized in the form of ultra-thin oblong plate shape after two-three weeks with a dimension of 128 ± 17 nm (length) × 14 ± 3 nm (width) and a thickness on the order of a few nanometers upon maturation (Fig. 2A and Fig. S2A-III, ESI†). In GO–CaP, the layer of GO microflakes was convolutely surrounded by CaP nanoparticles that experienced the same morphological elongation with maturation (Fig. 2B and Fig. S2B-I–III, ESI†). The freshly made or immature CaP and GO–CaP do not possess the enhancement effects on hMSC differentiation in subsequent experiments (data not shown).

Fig. 2C shows the representative Raman spectra from CaP, GO and GO–CaP. Raman spectrum from CaP indicated that the main component in CaP is hydroxyapatite with major Raman bands at 960 cm^{-1} (PO_4^{3-} ν1), 430 cm^{-1} (PO_4^{3-} ν2), and 589 cm^{-1} (PO_4^{3-} ν4).[6] The GO–CaP spectrum revealed the co-existence of GO and CaP, showing strong peaks from phosphate (430, 589, and 960 cm^{-1}) as well as the D band (1330 cm^{-1}) and G band (1597 cm^{-1}) from GO (Fig. 2C). The Ca/P ratio in the CaP molecules has been determined to be 1.20 ± 0.05 by inductively coupled plasma mass spectroscopy (ICP-MS), which is in agreement with the composition of calcium-deficient nonstoichiometric HAp.

To evaluate the materials' osteoinductive capability, GO, CaP and GO–CaP were introduced to hMSCs in osteogenic medium

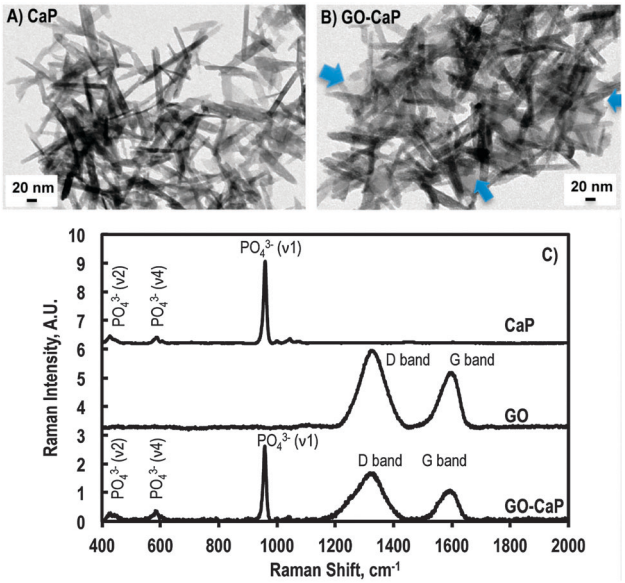

Fig. 2 TEM images of mature (A) CaP nanoparticles and (B) GO–CaP nanocomposites at 2 weeks after fabrication. Blue arrows on (B) point to the edge of underlying GO sheet. Scale bars indicate 20 nm. (C) Raman spectra from CaP, GO, and GO–CaP.

(OM) with a concentration of 0.5 μg ml^{-1}, 10 μg ml^{-1}, and 10.5 μg ml^{-1}, respectively. During the osteogenic differentiation of hMSCs, osteoblasts are generated and start to form bone nodules by producing extracellular calcium deposits. Mineralization was characterized using Alizarin red staining (ARS) after 2, 3, and 4 weeks of treatments. Cells in basic growth medium (GM) with treatments at all the time points were also tested as negative controls. The presence of calcium is indicated by red colour on the images (Fig. S3 in ESI†) and quantified by quantitative ARS assay (Fig. 3A). Calcium concentration was normalized to total protein content to account for possible variation in cell growth and proliferation.

Treatments with GO, CaP and GO–CaP in OM all induced significantly larger quantity of calcium than control at all the time points (Fig. 3A), while no calcification was observed in negative controls (with GM) (Fig. S3 in ESI†). GO–CaP nanocomposites exhibited superior osteoinductivity to CaP or GO, inducing much larger amount of mineralization than control. After 2 and 3 weeks, GO–CaP increased calcium deposition to levels more than 2 and 7 fold above those produced by CaP and GO, respectively. By 4 weeks, GO–CaP's calcium deposition exceeded that from other materials by $\sim 80\%$. In addition, the mineralization level with GO–CaP at 2 weeks was comparable to the control level at 4 weeks ($p > 0.05$), indicating GO–CaP significantly accelerated osteogenesis by two weeks. Phosphate assay was also performed from the deposition in parallel plates after 2 and 3 weeks of treatment. The amount of phosphate among all the groups follows the sequence of GO–CaP > CaP ≫ GO > control (Fig. S4 in ESI†), consistent with the outcome from calcium quantification.

Surprisingly, GO microflakes at this low concentration (0.5 μg ml^{-1}) increased calcification up to 50% more than the

Open Access Article. Published on 27 May 2014. Downloaded on 7/24/2025 2:59:40 AM.
This article is licensed under a Creative Commons Attribution 3.0 Unported Licence.

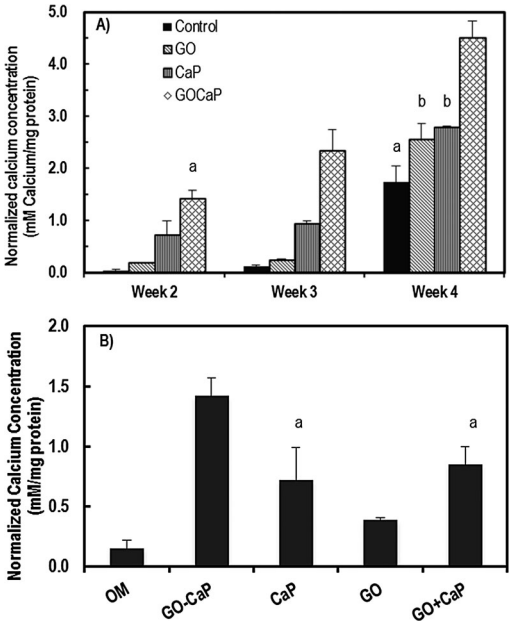

Fig. 3 (A) Normalized calcium concentrations determined by quantitative ARS assay of hMSCs after 2, 3 and 4 weeks of incubation with 0.5 μg ml^{-1} GO microflakes, 10 μg ml^{-1} CaP and 10.5 μg ml^{-1} GO–CaP. (B) Normalized calcium concentrations after 2 weeks treatment with 10.5 μg ml^{-1} GO–CaP, 10 μg ml^{-1} CaP, 0.5 μg ml^{-1} GO, and 0.5 μg ml^{-1} GO + 10 μg ml^{-1} CaP. Bars with the same top symbols indicate not being statistically significant ($p > 0.05$).

control at 3 and 4 weeks. At the late stage (4 weeks), the osteoinductivity of GO was comparable to the effect of CaP ($p > 0.05$). Such enhancement suggested that the GO flakes as 'free particles' preserved the osteoinductivity of GO coated supporting surface.

We further investigated whether the increased mineralization by GO–CaP is a simple addition effect of two individual osteoinductive compounds. First, the level of calcification in GO–CaP treated samples greatly exceeded the sum of those treated with GO and CaP individually (Fig. 3A). Next, separate experiments were carried out where hMSCs were incubated with the presence of both GO (0.5 μg ml^{-1}) and CaP (10 μg ml^{-1}) (GO + CaP) at the same concentration of individual components in 10.5 μg ml^{-1} GO–CaP in OM (Fig. 3B). GO + CaP induced increased calcification to the same extent as the effects of CaP ($p > 0.05$, Fig. 3B), which was still markedly outperformed by GO–CaP nanocomposites. These results indicate that GO–CaP as a new composite material possesses synergistic enhancement effect in osteogenesis compared to GO or CaP alone.

The osteogenic differentiation of hMSCs was verified through immunofluorescence staining of osteoblast markers alkaline phosphatase (ALP) and osteocalcin (OCN) after 2 weeks of treatments (Fig. 4). In good agreements with ARS assay, ALP activities and OCN expression level followed the sequence of GO–CaP > CaP ≫ GO > control, affirming the potential of GO–CaP in directing hMSCs differentiation toward osteogenic lineage.

The exact mechanism of GO and the derived composites in SCs differentiation is still unresolved. It has been generally

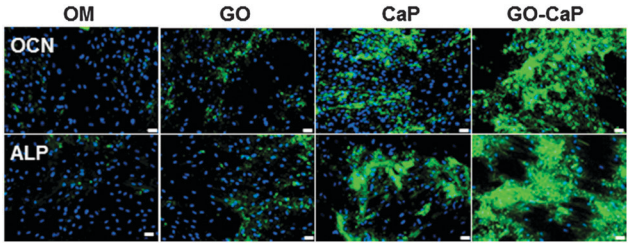

Fig. 4 Immunofluorescence staining of hMSC cell culture with FITC labeled (green) osteocalcin (OCN) antibody and DAPI (blue), and Alexa 488 (green) labeled alkaline phosphatase (ALP) antibody and DAPI (blue) after incubation with control osteogenic medium, GO, CaP, and GO–CaP for two weeks. Scale bars represent 20 μm.

hypothesized that the surface characteristics of graphene family nanomaterials such as nanotopography, surface stiffness, and large absorption capacity influence the molecular pathways that control the fate of stem cells.[7] Both G and GO were reported acting as preconcentrators for chemicals, proteins and growth factors on their surface to promote cell differentiation.[8] In GO–CaP, the surface of GO flakes was mostly covered by CaP nanoparticles, and thus was inaccessible for direct absorption of molecules. The enhanced differentiation may in part have arisen from the increased interaction between the intracellular focal adhesion complexes of the cells and the CaP structure on GO–CaP surface.[9] In addition, with the incorporation of GO and CaP, GO–CaP composites exhibited superior stiffness to GO or CaP alone.[10] Such increase in material stiffness could induce an enhanced mechanotransduction effect which has been recognized to regulate stem cell differentiation,[11] and thus might contribute to the synergistic enhancement in osteogenesis.

In conclusion, the present study synthesized a novel nanocomposite GO–CaP that possesses synergistic osteoinductive effect on hMSCs. To the best of our knowledge, only a couple of limited efforts have been made to develop composites with GO and CaP.[11] Besides differences in synthesis methods, nanoparticle composition, and morphology, none of the earlier studies evaluated the osteoinductivity of GO–CaP in hMSC differentiation. The GO–CaP nanocomposites fabricated in the current study significantly facilitated the osteogenesis of hMSCs and further enhanced calcium deposition by osteoblast. The exceptional osteoinductive properties of GO–CaP allow for its future application in regenerative medicine and bone tissue engineering.

The authors acknowledge National Institute of Health K25CA149194-01 (XB) for financial support.

Notes and references

1 (*a*) O. N. Ruiz, K. A. Fernando, B. Wang, N. A. Brown, P. G. Luo, N. D. McNamara, M. Vangsness, Y. P. Sun and C. E. Bunker, *ACS Nano*, 2011, **5**, 8100; (*b*) G. Y. Chen, D. W. Pang, S. M. Hwang, H. Y. Tuan and Y. C. Hu, *Biomaterials*, 2012, **33**, 418; (*c*) S. Ryu and B. S. Kim, *J. Tissue Eng. Regener. Med.*, 2013, **10**, 39; (*d*) G. Y. Chen, D. W. Pang, S. M. Hwang, H. Y. Tuan and Y. C. Hu, *Biomaterials*, 2012, **33**, 418.
2 (*a*) T. R. Nayak, H. Andersen, V. S. Makam, C. Khaw, S. Bae, X. Xu, P. L. Ee, J. H. Ahn, B. H. Hong, G. Pastorin and B. Ozyilmaz, *ACS Nano*, 2011, **5**, 4670; (*b*) J. Park, S. Park, S. Ryu, S. H. Bhang, J. Kim, J. K. Yoon, Y. H. Park, S. P. Cho, S. Lee, B. H. Hong and B. S. Kim, *Adv. Healthcare Mater.*, 2014, **3**, 176.

 This journal is © The Royal Society of Chemistry 2014

Open Access Article. Published on 27 May 2014. Downloaded on 7/24/2025 2:59:40 AM.
This article is licensed under a Creative Commons Attribution 3.0 Unported Licence.

3 (*a*) L. A. Tang, W. C. Lee, H. Shi, E. Y. Wong, A. Sadovoy, S. Gorelik, J. Hobley, C. T. Lim and K. P. Loh, *Small*, 2012, **8**, 423; (*b*) W. C. Lee, C. H. Lim, H. Shi, L. A. Tang, Y. Wang, C. T. Lim and K. P. Loh, *ACS Nano*, 2011, **5**, 7334; (*c*) J. Kim, K. S. Choi, Y. Kim, K. T. Lim, H. Seonwoo, Y. Park, D. H. Kim, P. H. Choung, C. S. Cho, S. Y. Kim, Y. H. Choung and J. H. Chung, *J. Biomed. Mater. Res., Part A*, 2013, **101**, 3520.

4 (*a*) Z. Wang, Z. Tang, F. Qing, Y. Hong and X. Zhang, *NANO*, 2012, **7**, 123004; (*b*) F. Habibovic and K. de Groot, *J. Tissue Eng. Regener. Med.*, 2007, **1**, 25; (*c*) S. Samavedi, A. R. Whittington and A. S. Goldstein, *Acta Biomater.*, 2013, **9**, 8037.

5 E. T. Hwang, R. Tatavarty, J. Chung and M. B. Gu, *ACS Appl. Mater. Interfaces*, 2013, **5**, 532.

6 X. Bi, C. A. Patil, C. C. Lynch, G. M. Pharr, A. Mahadevan-Jasen and J. S. Nyman, *J. Biomech.*, 2011, **44**(2), 297.

7 (*a*) M. Yang, J. Yao and Y. Duan, *Analyst*, 2013, **138**, 72; (*b*) M. Gu, Y. Liu, T. Chen, F. Du, X. Zhao, C. Xiong and Y. Zhou, *Tissue Eng., Part B*, 2014, DOI: 10.1089/ten.teb.2013.0638.

8 W. C. Lee, C. H. Lim, H. Shi, L. A. Tang, Y. Wang, C. T. Lim and K. P. Loh, *ACS Nano*, 2011, **5**, 7334.

9 (*a*) P. Müller, U. Bulnheim, A. Diener, F. Lüthen, M. Teller, E. D. Klinkenberg, H. G. Neumann, B. Nebe, A. Liebold, G. Steinhoff and J. Rychly, *J. Cell. Mol. Med.*, 2008, **12**, 281; (*b*) D. Depan, T. C. Pesacreta and R. D. K. Misra, *Biomater. Sci.*, 2014, **2**, 264; (*c*) K. van den Dries, M. B. M. Meddens, S. de Keijzer, S. Shekhar, V. Subramaniam, C. G. Figdor and A. Cambi, *Nat. Commun.*, 2013, **4**, 1412.

10 (*a*) M. Li, Y. Wang, Q. Liu, Y. Cheng, Y. Zheng, T. Xi and S. Wei, *J. Mater. Chem. B*, 2013, **1**, 475; (*b*) Y. Liu, J. Huang and H. Li, *J. Mater. Chem. B*, 2013, **1**, 1826.

11 (*a*) J. W. Shin, J. Swift, I. Ivanovska, K. R. Spinler, A. Buxboim and D. E. Discher, *Differentiation*, 2013, **86**, 77; (*b*) D. E. Discher, D. J. Mooney and P. W. Zandstra, *Science*, 2009, **324**, 1673; (*c*) J. S. Park, J. S. Chu, A. D. Tsou, R. Diop, Z. Tang, A. Wang and S. Li, *Biomaterials*, 2011, **32**, 3921; (*d*) J. Swift, I. L. Ivanovska, A. Buxboim, T. Harada, P. C. Dingal, J. Pinter, J. D. Pajerowski, K. R. Spinler, J. W. Shin, M. Tewari, F. Rehfeldt, D. W. Speicher and D. E. Discher, *Science*, 2013, **341**, 1240104.